COMPARISON OF MULTIPOLE EXPANSION AND EXACT FORM OF THE EDDY CURRENT FIELD OF THE AGS BOOSTER*

G.F. Dell, S.Y Lee, and G. Parzen

Brookhaven National Laboratory
Upton, NY 11973 USA

Abstract

Studies are made on magnetic field representation using a multipole expansion as well as the exact form to calculate the magnetic field produced by eddy currents in the vacuum chamber of the AGS Booster as well as the field produced by three turn correction coils attached to the top and bottom of the vacuum chamber. The multipole representation of the chamber field does not converge to the exact field when $X > 30$mm and limits the particle motion.[1] When the exact form of the chamber field is used, initial amplitudes in the horizontal plane (measured at QF) can be nearly as large as the chamber half aperture. Use of three turn correction coils to compensate the eddy current fields seems to reduce rather than increase the acceptance.

Introduction

Magnetic fields will be produced by eddy currents in the vacuum chamber of the AGS Booster. This field varies with B_{dot} and its importance changes during the acceleration cycle; in the present work we use $B_{dot}/B = 25$ sec^{-1} with $B = 0.3$ T. Although the vacuum chamber is made of inconel 625, has a resistivity $\sigma = 1.20 \times 10^{-6}$ Ωm, and a wall thickness of $d = 1.9$ mm (0.075 inches), in the present study the values $\sigma = 1.28 \times 10^{-6}$ Ωm $d = 2.0$ mm have been used.

The eddy current field is to be compensated by three turn coils attached to the top and bottom of the vacuum chamber. Figure 1 shows the first quadrant of the chamber cross section. The coils will be powered from a backleg winding on the dipole with a series resistor used to adjust the current to the desired value. This arrangement provides automatic compensation as the B_{dot} changes throughout the acceleration cycle.

Magnetic Field

Using the complex field notation of Beth[2] $H = H_y + iH_x$; the field produced at position $Z = X + iY$ by a current element I at $Z_c(k) = X_m(k) + iY_c(k)$ is:

$$H = I/4g \left(\tanh(\pi ZZ/2g) + \coth(\pi ZZ/2g) \right) \qquad (1)$$

where $ZZ = Z - Z_c(k)$. This expression is extended to the three turn correction coil and becomes:

$$\Delta B = \mu_0 I/4g \sum_{k=1}^{2} k \sum_{m}^{4} \left(\tanh(\pi ZZ/2g) + \coth(\pi ZZ/2g) \right) \qquad (2)$$

with $ZZ = Z - Z_c(k, m)$, $g = 82.55$ mm is the gap, the sum over k is made to describe the two coil positions as well as the different number of turns at the two positions, and the summation over m is used to include the contribution from each quadrant of the coil with:

$$Z_c(k,1) = -Z_c(k)^*,$$
$$Z_c(k,2) = -Z_c(k),$$
$$Z_c(k,3) = +Z_c(k), \text{ and}$$
$$Z_c(k,4) = +Z_c(k)^*$$

where $Z_c(k) = X_c(k) + iY_c(k)$ are the coordinates of the kth current element in the first quadrant, and $*$ denotes the complex conjugate. It is assumed that the field is a pure dipole at the origin. The nonlinear part of the coil field is obtained by subtracting the dipole field from the total field; the dependence of this field on transverse position in the magnet midplane is shown in Figure 2.
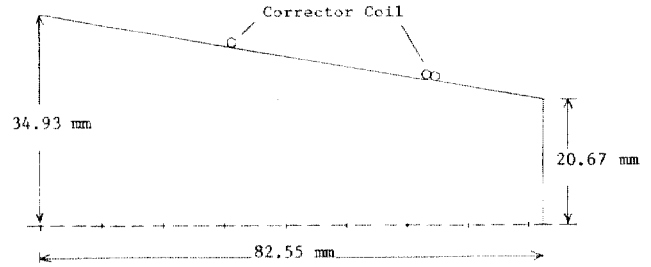

Figure 1: Axial view of the first quadrant of the Booster vacuum chamber. The first turn of the correction coil is located at $X = 31.75$ mm, $Y = 29.44$ mm, the other two are centered at $X = 63.50$ mm and $Y = 23.95$ mm. The surface of the vacuum chamber is given by $|Y| = -0.17283 |X| + 34.925$ mm.
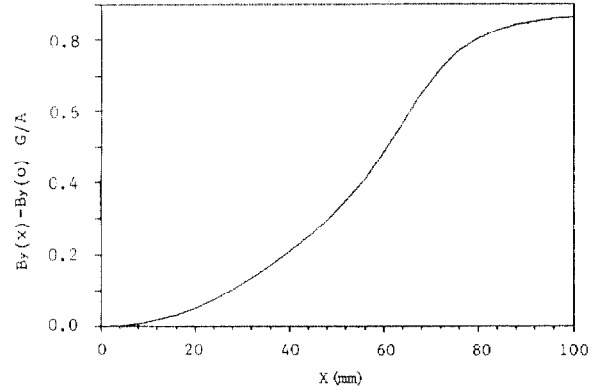

Figure 2: Midplane dependence of the nonlinear magnetic field from the 3 turn correction coils.

Chamber Field

The magnetic field produced by eddy currents in the vacuum chamber has also been evaluated using the exact form for finite current elements. In this case equation 2 is modified as follows:

$$\Delta B = \mu_0 I/4g \sum_{k=1}^{N_x} \sum_{m=1}^{4} \left(\tanh(\pi ZZ/2g) + \coth(\pi ZZ/2g) \right)$$
$$+ \mu_0 I/4g \sum_{k=1}^{N_y} \sum_{m=1}^{4} \left(\tanh(\pi ZZ/2g) + \coth(\pi ZZ/2g) \right) \qquad (3)$$

where $ZZ = Z - Z_c(k, m)$, μ_0 is the permeability of free space, $I = X_c \, d\ell \, dB_{dot}/\sigma$, the top section of the vacuum chamber shown
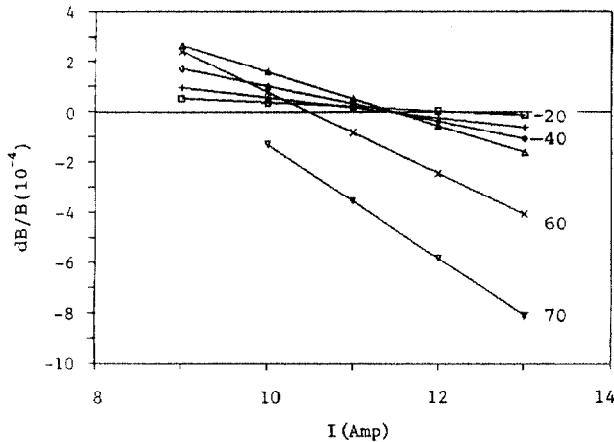
Figure 3: Dependence of the midplane field from the vacuum chamber and the correction coils on the corrector current. A corrector current of 11.4 A seems optimum.
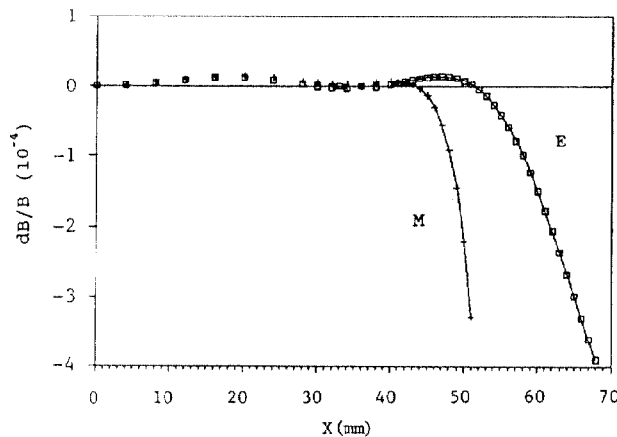

Figure 4: Dependence of $\Delta B/B$ on displacement in the chamber midplane. M denotes a chamber multipole expansion (corrector current $I = 11.25$ A), and E denotes the exact chamber field ($I = 11.4$ A).

in Figure 1 has been divided into N_x strips of width $d\ell = d\ell t$, and the side section has been divided into N_y strips of width $d\ell = d\ell s$. For the present study $N_x = 100$ and $N_y = 50$.

Multipole Expansion

The chamber field from the exact form has been expressed as a multipole expansion; the coefficients are listed in Table 1.

The calculation of the field from the vacuum chamber and the three turn correction coils has been incorporated in a stand alone program, and the dependence of the radial variation of the magnetic field has been determined both on and off the median plane. As expected, there is left-right symmetry of By and left-right plus up-down antisymmetry of Bx. The variation of $\Delta B/B$ when the chamber field is represented by the exact form or by a multipole expansion is determined at different transverse positions for several coil currents (Figure 3). A current is then selected that gives an acceptable variation of $\Delta B/B$ over the interval $0 \leq X \leq 50$ mm. For an assumed $B_{dot}/B = 25$, $B = 0.3$ T, resistivity $= 1.28 \times 10^{-6}\Omega$m, and 2 mm wall thickness, the optimum results are obtained when the current is 11.25 A with the multipole expansion and 11.4A with the exact form. The variation of the total field with displacement from the center of the vacuum chamber is shown in Figure 4. It is possible to reduce

Table 1: Multipole coefficients for chamber field.

n	$b_n \ (m^{-n})$
2	5.038×10^{-1}
4	4.813×10^{0}
6	-5.983×10^{3}
8	2.171×10^{6}
10	-1.269×10^{9}
12	3.606×10^{11}
14	-2.183×10^{15}
16	1.368×10^{17}

$\Delta B/B$ to $(+0.15, -0.04) \times 10^{-4}$ over the interval $0 < X < 50$ mm.

Particle Tracking

Lattice

The Booster lattice consists of six periods each containing four FODO cells. There is one dipole slot per half cell; the dipole slots in half cells three and six are empty giving 36 dipoles in the lattice. Chromaticity correction is achieved with two families of sextupoles, SF and SD, placed adjacent to the QF and QD quadrupoles, respectively. Sextupoles are present in all half cells; there are 48 sextupoles in the lattice. In the present study the chromaticity is corrected to zero. When the multipole expansion is used for the chamber field, the chromaticity contribution from the b_2 coefficients is included and corrected. When the correction coils are used with the exact form of the chamber field, the assumption is made that the sextupole fields cancel, and only the natural chromaticity is corrected by the SF and SD sextupoles. The chromaticities and sextupole strengths are listed in Table 2. The betatron tunes are $Qx = 4.820$, $Qy = 4.823$.

Table 2: Chromaticity and sextupole strengths $(\zeta_x = \zeta_y = 0)$.

	Exact Form		Multipole Expansion	
	Natural Chrom.	Integrated Strength	Chrom. with b_2	Integrated Strength
X	-5.093	-0.18218	0.239	-0.09023
Y	-5.447	0.29495	-10.431	0.42166

Simulation

The program for the field calculation has been incorporated into a version of the PATRICIA tracking program with the corrector current being defined in the input. Options are given to allow tracking with the following conditions:

1. Chamber (multipole expansion),
2. Chamber (exact form),
3. Chamber (multipole) + correction coils (exact),
4. Chamber (exact) + correction coils (exact).

During tracking the $\Delta B/B$ at the center and ends of each dipole are determined, and the particles are given a kick with $\Delta B\ell/B\rho$ weighted according to a three point Simpson rule. The computer time (CRAY XMP) required for tracking with the exact form of the chamber field is large; the time per particle turn is 2.25 ms for the chamber multipole expansion only, 10 mS for the chamber multipole expansion plus the exact calculation of the three turn correction coils, and 636 ms when the exact forms are used for the chamber (Nx=100 and Ny=50) and the correction coils. Originally the field determination with the exact form was made with Nx=1000 and Ny=1000. This is prohibitive for tracking; reducing the number of current elements to Nx=100 and Ny=50 per quadrant does not seriously effect the description of the magnetic field. Furthermore, the tracking runs were reduced from 1000 turns to 400 turns.

Motion for which the particle amplitude exceeds the chamber dimensions is meaningless and consumes computer time; consequently a test is made at each dipole to assure that the test

particle is within the vacuum chamber. For a particle at position (X,Y), the surface of the vacuum chamber is determined from $Y_{ch} = -0.17283|X| + 34.925$, and tests are made to assure that $|Y| \leq Y_{ch}$ and $|X| \leq 82.55$ mm.

A detailed study has been made for horizontal amplitudes at the QF quadrupoles between 10mm and 80mm ($\Delta x = 10$mm). Particles are launched with ($X \neq 0$, $Y \neq 0$, $X' = 0$, and $Y' = 0$) or ($X \neq 0$, $Y = 0$, $X' = 0$, and $Y' \neq 0$). The vertical emittance is increased in increments corresponding to $\Delta Y = 1$mm at a QD until the particle motion exceeds the dimensions of the vacuum chamber; the average of the pass/fail amplitudes is used as a measure of the vertical aperture, and the smaller of the measurements from the two launching conditions is used to determine the acceptance. In general, the first launching condition causes emittance transfer from the vertical to horizontal plane, and the second causes emittance transfer from the horizontal to vertical plane and thus limits the acceptance. Figure 5 shows the results when the chamber field is represented by the multipole expansion; the point of observation is at the end of the dipole near the defocusing quadrupole where the horizontal size is minimum and the vertical size is maximum. Larger horizontal displacements are possible when the correction coils are not powered than when they are powered.

The results for the exact form plus correction coils are shown in Figure 6. As before, the correction coils seem to decrease the acceptance. In this case particles having horizontal amplitudes of 80mm, measured at the center of the QF quadrupoles, survive throughout the tracking run.

The acceptance profile at other locations can be determined by scaling the results shown in Figures 5 & 6 by the ratios of the $\sqrt{\beta}$ functions; these ratios are listed in Table 3 for the center of the QF and QD quadrupoles as well as at the two ends of the dipoles, BQF and BQD.

Table 3: Scale factors for translating X and Y.

	QF	BQF	BQD	QD
β_x	13.16	9.44	4.18	3.64
β_y	3.70	5.41	12.04	13.64
X/X_o	1.77	1.50	1.00	0.93
Y/Y_o	0.55	0.67	1.00	1.00

Results

The present study indicates that a field representation by a multipole expansion for a noncircular geometry diverges and gives results that are pessimistic. Use of the exact form for the field representation predicts larger acceptances. In both cases the inclusion of the correction coils reduces the acceptance rather than increasing it. Runs have been made with the current in the correction coils reversed to verify they are corrected properly; this configuration further reduces the acceptance. Runs were also made with no field from the chamber or the correction coils; in this case the acceptance was increased and provides a check that the chamber field affects the particle motion.

A previous study made when the field of the correction coils was represented by a multipole expansion (rather than the exact form) showed the field description was not valid for displacements exceeding the radius of the coils. At small displacements the multipole expansion could be expected to be somewhat valid – the presence of multipoles with order higher than sextupoles leads us to surmise that the exact field from the correction coils also has higher order components and that these limit the acceptance.

Coupling with transfer of emittance between the horizontal and vertical planes is modest when chromaticity correcting sextupoles are included in all half cells of the lattice. The direction

of the emittance coupling (horizontal to vertical or vertical to horizontal) depends on the launching conditions of the test particle. Two launching conditions have been used, and the smaller of the two results is reported. Tracking with the first launching condition indicates there is little emittance transfer from the horizontal to the vertical plane, while the second launching condition shows a 10–15% transfer of emittance from the horizontal to the vertical plane – this becomes important when $\epsilon_x > \epsilon_y$ and causes a reduction of the acceptance.

References

1. S.Y. Lee, BNL Internal report AD/AP/TN-12, Sept. 1989.

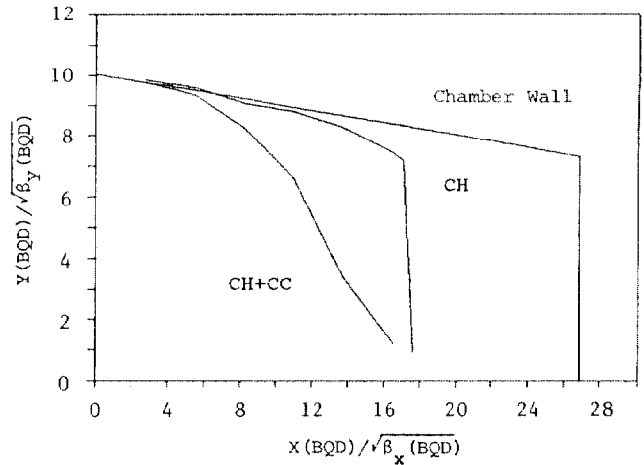2. R.A. Beth, J. Appl. Phys. 39, 2568(1968).

Figure 5: Tracking results showing the maximum initial vertical amplitude for horizontal displacements $10 \leq X \leq 80$ mm (at QF) when the chamber field is represented by the multipole expansion. Point of observation is the dipole end nearest the QD quadrupoles. CH denotes chamber only, and CH+CC denotes chamber plus correction coils.
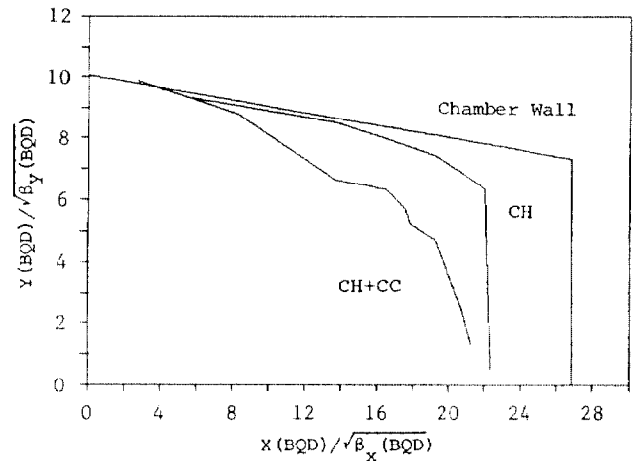

Figure 6: Tracking results showing the maximum initial vertical amplitude for horizontal displacements $10 \leq X \leq 80$ mm (at QF) when the exact form is used for the chamber field. CH denotes chamber only, and CH+CC denotes chamber plus correction coils.